LAWRENCE
LIVERMORE
NATIONAL
LABORATORY

UCRL-CONF-232590

ODTX Measurements and Simulations on Ultra Fine TATB and PBX-9502

Jake Koerner, Jon Maienschein, Alan Burnham, Aaron Wemhoff

July 9, 2007

North American Thermal Analysis Society 35th Annual Conference
East Lansing, MI, United States
August 26, 2007 through August 29, 2007

Disclaimer

ODTX Measurements and Simulations on Ultra Fine TATB and PBX-9502

Jake Koerner*, Jon Maienschein, Alan Burnham, Aaron Wemhoff
Lawrence Livermore National Laboratory
7000 East Avenue L-282
Livermore, CA 94550
koerner2@llnl.gov

ABSTRACT

We measure the time to explosion of 12.7 mm diameter spheres of ultra fine TATB and PBX-9502 (95 wt% TATB, 5 wt% Kel-F 800) at 85.0, 92.5, and 98.0 percent of theoretical maximum density (TMD) in confined and unconfined configurations and at several elevated temperatures with the Lawrence Livermore National Laboratory (LLNL) One Dimensional Time to Explosion (ODTX) apparatus. Time to explosion data provide insight into the relative ease of thermal ignition and allow for the calibration of kinetic parameters. The measurements show that PBX-9502 is more thermally stable than ultra fine TATB, that unconfined samples are slightly more thermally stable than confined ones, and that lower density samples are more thermally stable than higher density ones. "Go/no go" data at the lowest temperatures yield an experimental measurement of the critical temperature, which is the temperature at which an explosive can be heated indefinitely without undergoing self-heating and concomitant rapid and violent decomposition. Critical temperatures ranges for 12.7 mm diameter spheres of 98% TMD ultra fine TATB and PBX-9502 are 213-230 °C and 234-239 °C, respectively. Experimental data are modeled with ALE3D and kinetic parameters are determined. These kinetic parameters, when coupled with thermal property data, provide good prediction of the time to explosion.

INTRODUCTION

Measurement and prediction of the time to explosion as a function of temperature for a finite body of exothermically reacting material is of broad interest for industrial and military applications. We at LLNL are primarily interested in these measurements and predictions on energetic materials, namely, high explosives (HE). Time to explosion measurements have been made on a wide variety of HEs using the LLNL ODTX apparatus. The ODTX apparatus was first reported in 1976 by Catalano (1). A new system, which is geometrically identical to the old one, but incorporates new components, modern equipment, and expanded diagnostic capabilities, was deployed in 2001 and is used in this work (2).

EXPERIMENTS AND CALCULATIONS

LLNL ODTX Apparatus

ODTX experiments measure times to explosion and minimum ignition temperatures of high explosives. These measurements provide insight into the relative ease of thermal ignition and allow for the determination of kinetic parameters. The experiment involves isothermally heating a 12.7 mm diameter spherical sample in a 12.7 mm diameter spherical cavity between two aluminum anvils. The apparatus is pictured in Figure 1 and key components are labeled.

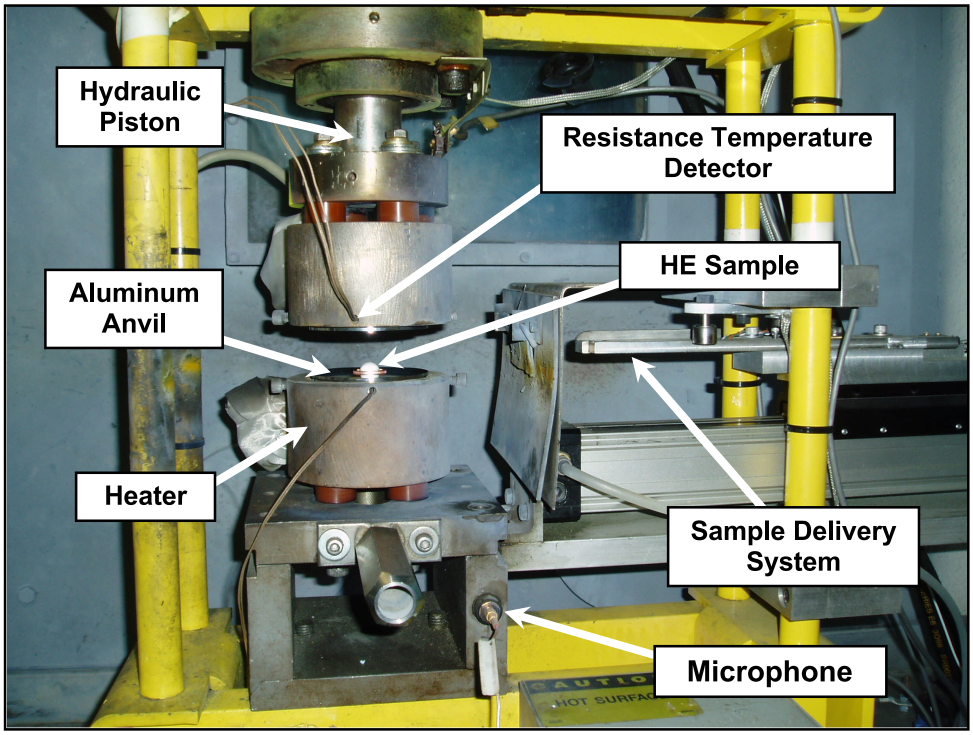

Figure 1. LLNL ODTX apparatus with key components labeled.

The sample is remotely delivered to the anvil cavity with the sample delivery system. A cross-sectional view of the anvil cavity is shown in Figure 2.

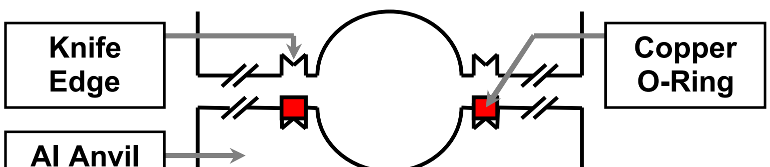

Figure 2. Cross-sectional view of 12.7 mm diameter spherical anvil cavity.

The hydraulic piston drives the top heater and anvil downward towards the bottom heater and anvil. A copper o-ring, if present, provides approximately 150 MPa of confinement pressure when the two knife-edges on the aluminum anvils compress it. The top and bottom anvil temperatures are recorded to 0.1 °C by resistance temperature detectors and a microphone measures a sound signal which indicates the time at which an explosion occurs. The sample is heated by the anvils until it violently reacts.

<u>Materials</u>

The ultra fine TATB used is 100% ultra fine TATB while the PBX-9502 is 95 wt% dry aminated TATB and 5 wt% Kel-F 800. Particle sizes for ultra fine TATB and dry aminated TATB are 3.8 and 70 μm, respectively (3). LLNL lot identification numbers for ultra fine TATB and PBX-9502 are C-295 and C-382, respectively.

Both materials were uniaxially pressed in a spherical mechanical pressing die at 207 MPa (30,000 psi) and at 105 °C to densities of 85.0, 92.5, and 98.0% TMD. Ultra fine TATB and PBX-9502 TMDs are 1.940 and 1.943 g/cm^3, respectively.

ALE3D Calculations

The Arbitrary Lagrangian-Eulerian in Three Dimensions (ALE3D) computer code is used in many LLNL applications to predict both the timing and violence of thermal ignition events (4). ALE3D includes the calculation of chemical reactions, thermal transport, and material movement and deformation. Most previous applications of ALE3D have used chemical reactions that exhibit Arrhenius temperature dependence and that depend on the concentration of one or more materials to the n^{th} power, where n is an integer. Recently, an autocatalytic model adapted from Prout and Tompkins was installed into ALE3D, since explosives tend to have autocatalytic mechanisms (5). The equation states

$$\frac{dx}{dt} = -kx^n (1 - qx)^m \tag{1}$$

where

$$k(T) = A \exp\left(-\frac{E}{RT}\right) \tag{2}$$

and

x = mass fraction of reactant remaining
A = frequency factor
E = the activation energy
R = universal gas constant
T = temperature
n, m, q = Prout-Tompkins model parameters

This model has been applied successfully to HMX cookoff (6). Here, we apply it to ultra fine TATB and PBX-9502 to determine kinetic parameters A and E.

RESULTS AND DISCUSSION

ODTX Experimental Results

ODTX test results for ultra fine TATB and PBX-9502 are shown in Figures 3 and 4. Because times to explosion are fairly reproducible, some data overlap. Raw time to explosion data are included in the Appendix for clarity. For each experiment, sample density, confinement, and temperature are varied.

Observation of post-shot anvils indicates that the presence of the copper gasket may not completely confine the sample in some cases, especially at higher temperatures. Post-shot anvil images of different confinement scenarios are shown in Figure 3 to illustrate this.

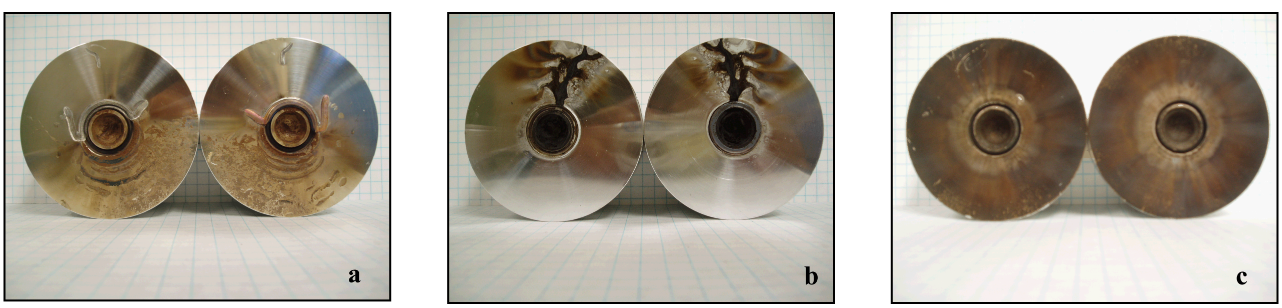

Figure 3. Post-shot anvil images illustrating a) successful confinement b) possible failed confinement c) no confinement

Figure 3.a shows successful confinement. Part of the copper gasket is seen outside the anvil cavity, and its impression is seen on that anvil's pair. When the explosion occurs, rapidly expanding gas pushes the anvils apart and the copper gasket away from the anvil cavity. Once the gas escapes, the anvils, still under pressure, rapidly close. Figure 3.b shows an intact copper gasket and a channel

leading from the anvil cavity across the anvil surface. Here, it appears as if the copper gasket failed not by rupture, but by the formation of a hole between the anvil surface and the copper gasket. If the hole forms near the end of the experiment or if it is small in size, decomposition gasses escape very slowly, and confinement exists. However, if the hole is large or forms near the beginning of the experiment, a larger volume of decomposition gasses may leak, and confinement may not exist. In Figure 3.c, no copper gasket is present during the experiment, and a dark, thin coating of reacted explosive residue is seen on the anvil surface.

These three images are characteristic of all ultra fine TATB and PBX-9502 confinement scenarios. Data tabulated in the Appendix from runs which were confined, but do not show gasket rupture, as in Figure 3 are marked with an asterisk.

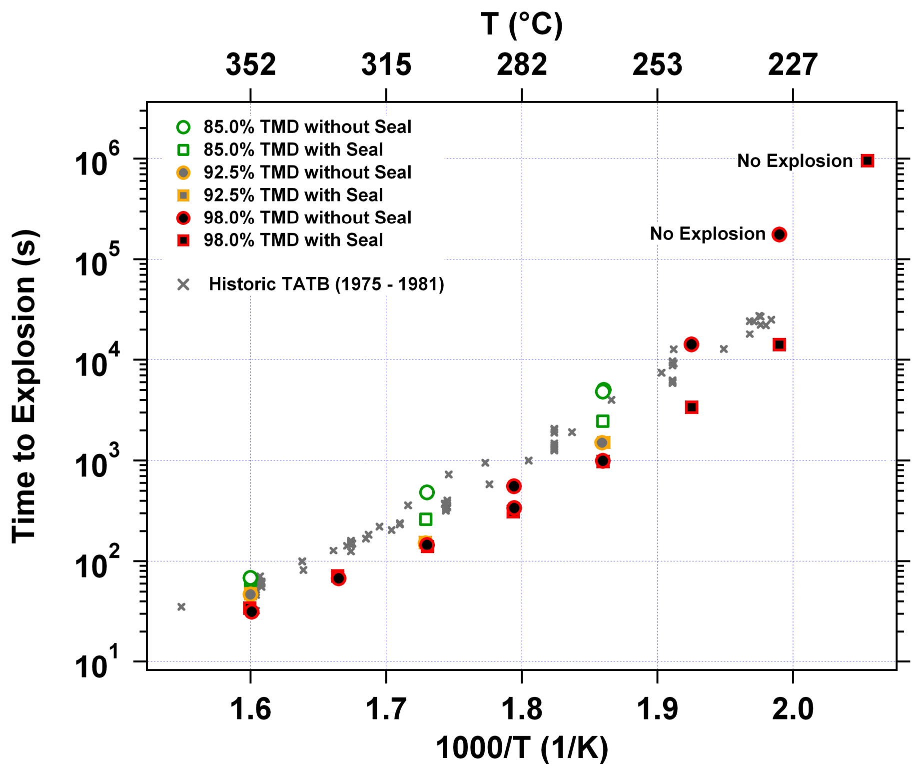

Figure 3. ODTX data for ultra fine TATB

In general, ultra fine TATB exhibits shorter times to explosion than historic TATB. Some systematic error is present in the historic TATB data, as historic TATB and ultra fine TATB were tested on two different apparatuses. Tran showed that the temperature in the center of the cavity of the apparatus used to test historic TATB is 2-3°C lower than that of the new apparatus; however, if the historic data are corrected for this difference, the result is only a 0.01 1/K shift to the right of the historic TATB data. Also, one might expect a lower differential scanning calorimetry (DSC) exotherm onset temperature for historic TATB to explain the differences in times to explosion. While no DSC data could be located from historic TATB lots, DSC data on similarly formulated TATB does exist and does not vary significantly from that of ultra fine TATB. Unless the historic TATB lots are significantly different than the ones for which DSC data exists, some other phenomena are causing the reduction in time to explosion of ultra fine TATB.

Ultra fine TATB times to explosion increase as temperature, sample density and confinement decrease. Increases in time to explosion due to reduced density and confinement seem to be more pronounced at lower temperatures.

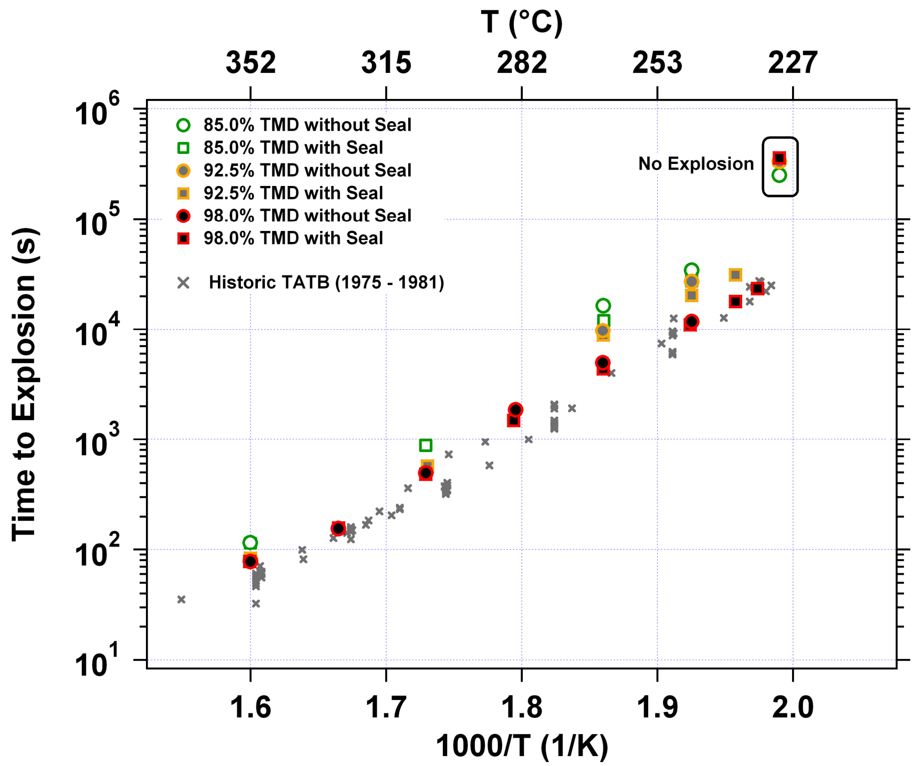

Figure 4. ODTX data for PBX-9502

In general, PBX-9502 exhibits longer explosion times than historic TATB. The presence of 5 wt% Kel-F 800 binder is one likely contributor. Tarver suggests that the longer thermal explosion times for plastic bonded explosives with endothermic binders are most likely due to endothermic reactions of the binders with the gaseous decomposition products of the high explosive (7). Increases in times to explosion due to decreased density and confinement for PBX-9502 are similar to those of ultra fine TATB.

Historically, ODTX measurements have been conducted at temperatures high enough to cause the test material to violently react within three hours. For these experiments, we test at lower temperatures and thereby extend the heating time of the test material to up to 11 days. The benefits of this test method are two fold. First, kinetic parameters used in ALE3D computer codes to fit ODTX data can be more accurately calibrated. Second, we gain insight into the critical temperature, which is the temperature at which an explosive can be heated indefinitely without undergoing self-heating and concomitant rapid and violent decomposition. The critical temperature ranges were determined to be 213-230 °C and 234-239 °C for 98% TMD ultra fine TATB and 98% TMD PBX-9502, respectively. It is important to note that critical temperature is geometry dependent, and that these values are reported for 12.7 mm diameter spherical samples tested in sealed configurations.

ALE3D Modeling Results

We reported experimental times to explosion on ultra fine TATB and PBX-9502 pressed to various densities and tested in sealed and unsealed configurations. We calibrate kinetic parameters and compare modeling results to experimental results using the ALE3D computer code. To calculate times to explosion in ALE3D, thermal conductivities and heat capacities of the materials are needed. Thermal conductivities were calculated using an ALE3D thermal conductivity estimator tool and heat capacities were calculated by mass averaging material components. The values are shown in Table 1 (8).

Table 1. Thermal transport properties for ultra fine TATB and PBX-9502 at various densities

Material	%TMD	Density	Heat Capacity	Thermal Conductivity	Thermal Diffusivity x 10^6
		(g/cm^3)	(J/kg·K)	(W/m·K)	(m^2/s)
ultra fine TATB	98.0	1.9012	1000.1	0.522	0.275
	92.5	1.7945	1000.5	0.466	0.260
	85.0	1.6490	1001.1	0.395	0.239
PBX-9502	98.0	1.9041	1100.5	0.563	0.269
	92.5	1.7973	1095.3	0.500	0.254
	85.0	1.6516	1088.1	0.412	0.229

The ALE3D results for ultra fine TATB and PBX-9502 in sealed configurations are shown in Figures 5 and 6, respectively.

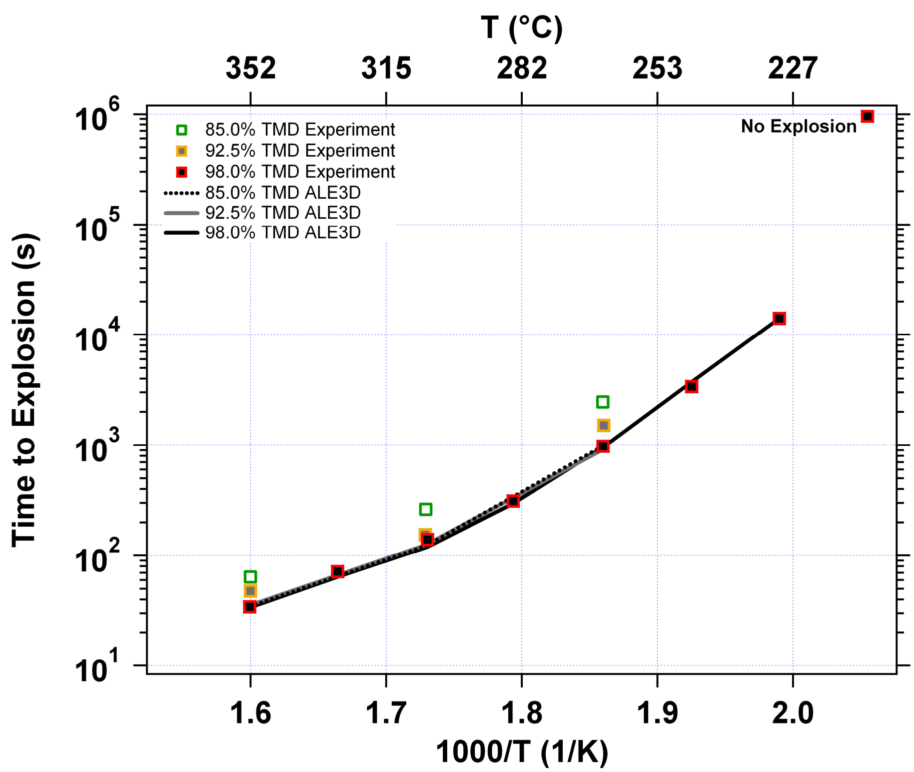

Figure 5. ODTX data and ALE3D modeling results for ultra fine TATB in sealed configuration

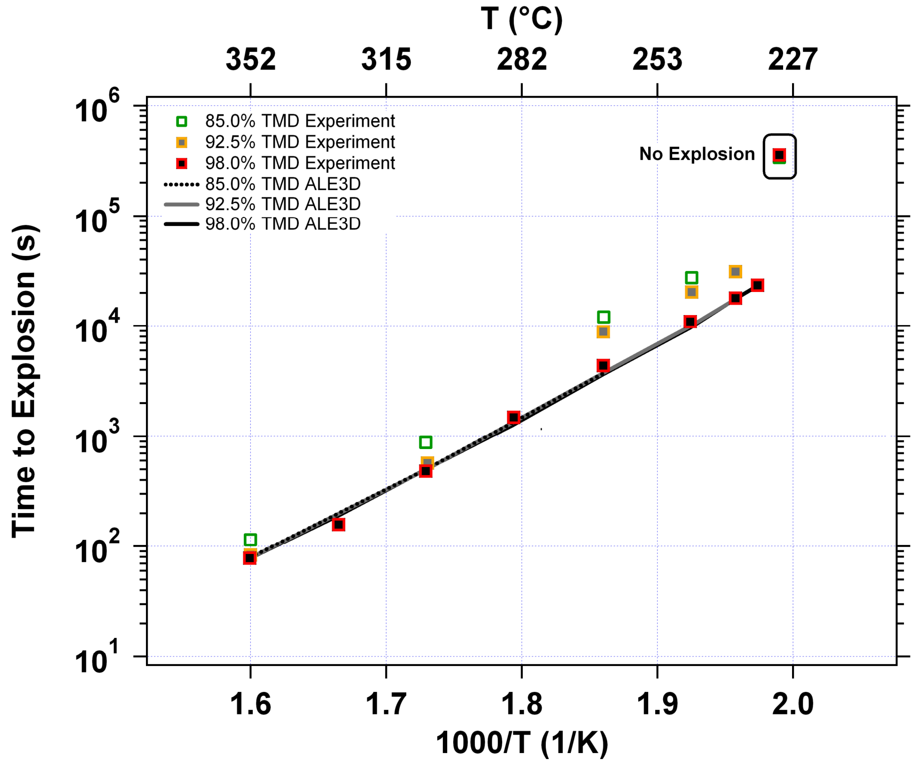

Figure 6. ODTX data and ALE3D modeling results for PBX-9502 in sealed configuration

ALE3D modeling results for 98% TMD materials fit the experimental data well, as they should. 98% TMD data were used to calibrate the kinetic parameters. The ALE3D curves for 92.5 and 85.0% TMD samples essentially overlap the 98% TMD curve and do not fit the experimental data as well. One reason that the reduced density does not seem to affect the time to explosion calculated by ALE3D is because the reduced density is counterbalanced by a lower thermal conductivity. This results in only a modest change in thermal diffusivity and, consequently, only a modest change in heat transfer into the sample (9). Also, if TATB kinetics are pressure dependent, the ALE3D code may not be modeling them properly. Consider that as TATB is heated, it slowly generates decomposition gases. For 92.5 and 85.0% TMD samples, significant void space exists and may allow for additional decomposition gas generation inside the anvil cavity. If kinetics are pressure dependent, the additional void space and subsequent reduction in pressure would slow reactions leading to further decomposition and eventual explosion.

For unconfined samples, the void space is essentially infinite, so an increase in time to explosion is also expected for this test configuration.

Frequency factors, activation energies, Prout-Tompkins parameters, critical temperature calculations, and average fit errors are determined from the ALE3D fits to the 98% TMD ultra fine TATB and PBX-9502 curves and shown in Table 2 below.

Table 2. ALE3D-determined frequency factors, activation energies, Prout-Tompkins parameters, and critical temperatures

	A (1/s)	**E/R (K)**	**m/n/q (d'less)**	**$T_{critical}$ (°C)**	**Average Fit Error (%)**
ultra fine TATB	$2.41 \cdot 10^9$	15389	0.656/1/0.999999	221	6
PBX-9502	$1.85 \cdot 10^{10}$	15618	1/1/0.999999999	199	9

Literature values for E/R for ultra fine TATB and PBX-9502 based on DSC data are reported as 24176 and 23214 K, respectively (10). It is important to note that these values are reported for smaller samples at different pressures, in a different test configuration, and using different kinetic analysis techniques, so some variation is expected.

SUMMARY AND CONCLUSIONS

We measured the time to explosion of 12.7 mm diameter spheres of PBX-9502 and ultra fine TATB at 85.0, 92.5, and 98.0% TMD in confined and unconfined configurations and at several elevated temperatures with the LLNL ODTX apparatus. These measurements provided insight into the relative ease of thermal ignition. In general, thermal stability increases as temperature, density, and confinement decrease. These experiments also allowed for the determination of kinetic parameters used in the Prout Tompkins equation. The experiments and modeling techniques described can be applied to a wide variety of energetic materials and will continue to provide valuable insight into their thermal response behavior.

ACKNOWLEDGEMENTS

We gratefully acknowledge Sally Weber, Greg Sykora, and Dan Greenwood for their contributions to this experimental effort.

This work was performed under the auspices of the U.S. Department of Energy by University of California, Lawrence Livermore National Laboratory under contract W-7405-Eng-48.

REFERENCES

1. E. Catalano, R. McGuire, E.L. Lee, E. Wrenn, D. Omellas, and J. Walton, *Sixth International Symposium on Detonation Proceedings*, 1995, p. 214, Office of Naval Research, ACR-221, Coronado, CA.
2. T.D. Tran, R.L. Simpson, J.L. Maienschein, C. Tarver, Thermal decomposition of trinitrotoluene (TNT) with a new one dimensional time to explosion apparatus, *32nd International Annual Conference of Institute of Chemistry Technology*, 2001, UCRL-JC-141597.
3. M.D. Hoffman, A.R. Mitchell, S.C DePiero, Characterization of new TATBs, In Preparation for Print, 2007
4. J.J. Yoh, M.A. McClelland, J.L. Maienschein, J. F. Wardell, C.M. Tarver, Simulating thermal explosion of cyclotrimethylenetrinitramine-based explosives: model comparison with experiment, *J. Appl. Phys.*, 2005, 97, 083504.
5. Burnham A.K., Application of the Sestak-Berggren equation to organic and inorganic materials of practical interest. *J. Them. Anal. & Cal.*, 60, 895-908.
6. A.P. Wemhoff, A.K. Burnham, A.L. Nichols, Application of global kinetic models to HMX β-δ transition and cookoff processes, *J. Phys. Chem.* 2007, 111, 1575-1584.
7. C.M. Tarver, J.G. Koerner, Effects of endothermic binders on HMX- and TATB-based plastic bonded explosives, accepted for publication in *Journal of Energetic Materials*, 2007.
8. LLNL Online Explosive Reference Guide, April 2007 Edition, UCRL-WEB-230075
9. F.P. Incropera, D.P. DeWitt, *Fundamentals of Heat and Mass Transfer*, 5th Edition, 2002, Wiley.
10. R.K. Weese, A.K Burnham, H.C. Turner, T.D. Tran, Exploring the physical, chemical and thermal characteristics of a new potentially insensitive high explosive RX-55-AE-5, *Journal of Thermal Analysis and Calorimetry*, 2007, 89, 465-473

APPENDIX: Raw ODTX Data

Material	TMD	Confinement	Temperature	1000/T	Time
	(%)	(Yes/No)	(°C)	(1/K)	(s)
Ultra Fine TATB	85.0	Yes	351.9	1.59987	64.147*
			305.2	1.72906	262.861
			264.6	1.8596	2469.79*
		No	351.9	1.59987	68.419
			264.4	1.86029	5035.26
			264.6	1.8596	4833.12
			304.9	1.72995	485.613
	92.5	Yes	305.3	1.72876	154.963*
			351.9	1.59987	47.772
			264.4	1.86029	1515.43*
		No	264.75	1.85908	1503.85
			351.9	1.59987	46.822
			305.25	1.72891	152.692
	98.0	Yes	304.75	1.7304	140.151*
			352.15	1.59923	34.399*
			264.55	1.85977	976.505
			284.4	1.79356	312.808
			327.75	1.66417	71.709*
			246.3	1.92511	3397.5
			229.4	1.98985	14096.1
			213.5	2.0549	955390**
		No	304.9	1.72995	146.333
			327.5	1.66486	67.65
			351.6	1.60064	31.694
			284.25	1.79404	555.874
			264.6	1.8596	993.584
			284.15	1.79437	340.469
			246.35	1.92493	14173.1
			229.4	1.98985	176079**
PBX-9502	85.0	Yes	351.95	1.59974	115.147*
			305.2	1.72906	880.741
			264.4	1.86029	12106.6
			246.3	1.92511	27496.4
			229.4	1.98985	338659**
		No	264.5	1.85995	16464.6
			352	1.59962	116.717
			246.3	1.92511	34342.8
			229.4	1.98985	250009**
	92.5	Yes	351.9	1.59987	83.394*
			304.75	1.7304	570.338*
			264.5	1.85995	8869.35*
			246.3	1.92511	20405.7
			237.7	1.95752	31216.7
		No	351.9	1.59987	81.857
			264.6	1.8596	9773.05
			246.3	1.92511	27230.1
			229.4	1.98985	331833**
	98.0	Yes	352.15	1.59923	77.95*
			327.5	1.66486	158.069*
			305.2	1.72906	484.008*
			284.3	1.79388	1488.77
			264.5	1.85995	4382.37
			246.55	1.92419	10974.1
			229.4	1.98985	356159**
			237.7	1.95752	17976
			233.5	1.97375	23540
		No	351.9	1.59987	78.313
			327.6	1.66459	156.809
			305.2	1.72906	495.842
			283.85	1.79533	1866.68
			264.6	1.8596	4971.16
			246.3	1.92511	11864.4

* possible failed confinement ** no explosion, represents time at which experiment was aborted